

SFDM: A new formation mechanism of tidal debris

Victor H. Robles*, L. A. Martinez-Medina and T. Matos

Departamento de Física, Centro de Investigación y de Estudios Avanzados del IPN, AP 14-740, 0700 D.F., México

26 March 2022

ABSTRACT

Recent observations of tidal debris around galaxies have revealed that the structural properties of the spheroidal components of tidally disturbed galaxies are similar to those found in non-interacting early-type galaxies (ETGs), likely due to minor merging events that do not strongly affect the bulge region or to major mergers that happened a long time ago. We show that independently of merger events, tidal features like shells or rings can also arise if the dark matter is an ultra light scalar field of mass $\sim 10^{-22} \text{eV}/c^2$. In the scalar field dark matter (SFDM) model the small mass precludes halo formation below $\sim 10^8 M_\odot$ reducing the number of small galaxies today, it produces shallow density profiles due to the uncertainty principle in contrast to the steep profiles found in the standard cold dark matter (CDM) paradigm, in addition to the usual soliton solution there exists dark matter haloes in multistates, characterized by ripples in their density profiles, which are stable provided that most of the halo mass resides in the ground state. We use the hydrodynamics code ZEUS to track the gas evolution in a background potential given by a superposition of the ground and first excited state of the scalar field, we study this configuration when it is initially unstable (excited state more massive than ground state) but by a population inversion in the states it eventually becomes stable, this could happen when haloes decoupled from the expansion of the universe and collapse to reach a state of equilibrium. We found that tidal structures like rings are formed at a particular radius as a direct consequence of the wavelike structure of the dark matter halo, thus they possess a certain degree of symmetry that can be used to distinguish them from remnants formed through the usual galaxy merging mechanism. In our simulations most of the gas concentrates in the center of the halo forming a dense and compact structure likely enhancing star formation in this region, however, some of the gas always remains trapped between the overdensity regions of the background SFDM halo predicting surrounding features even in non-interacting galaxies. In galaxies that are not strongly interacting with their neighbors, these structures may leave traces such as radial gradients in stellar metallicity, rings of dust, or even in the form of a younger population of stars at particular radii in contrast to the old stellar population dominating the bulge region, our results offer a new mechanism in which features like rings and shells can emerge purely from the quantum properties of this ultra light scalar field.

Key words: circumstellar matter – infrared: stars.

1 INTRODUCTION

The standard model of cosmology (or CDM) assumes that the dark matter (DM) is cold and effectively collisionless. It assumes a hierarchical framework for galaxy formation and throughout their evolution galaxies are subject to frequent collisions and interactions with nearby galaxies that leave surrounding material in the form of tidal debris, therefore

studying tidal features can yield important clues on galaxy evolution.

Tidal features can appear in the form of complicated structures (Barnes & Hernquist 1992), but it is frequent to observe structures like tidal tails around the bulge of massive galaxies (Fort et al. 1986; Bendo et al. 2006), some early-type galaxies present shells (Malin & Carter 1980, 1983; Turnbull, Bridges & Carter 1999; van Dokkum 2005; Schweizer & Seitzer 1992; Michard & Prugniel 2004) which can be seen as smooth arcs of ellipses centered around its host galaxy decreasing their surface brightness for

* E-mail: vrobles@fis.cinvestav.mx

larger radii, there are also debris in the form of stellar streams (Martínez-Delgado et al. 2008, 2009, 2010).

Several analyses of the spheroidal components of tidally disturbed early-type galaxies (ETGs) (Taehyun et al. 2012) suggest that structural properties such as the effective radius (radius at which half of the total light of the system is emitted) and their surface brightness are quite similar from those of the other ellipticals or the spheroids of galaxies with few or no signs of tidal interaction. Other results have shown evidence of kinematically decoupled components in early-type galaxies (Hau & Duncan 2006; Koprolin & Zeilinger 2000). Given the standard paradigm of CDM it is expected that even these “passive” galaxies also formed by galaxy mergers, then the similarity of the bulge regions for the ETGs could be due to the some minor mergers (galaxy mergers of unequal mass with mass ratio of $1/10 - 1/100$) slightly affecting the bulge but massive enough to still induce tidal debris, or by major mergers (mergers of comparable mass galaxies) that happened a long time ago so that now the bulge has relaxed. Cosmological N-Body simulations in CDM have shown (Klypin et al. 2011; Behroozi et al. 2011) that merger events are frequent when galaxies are growing, however, it must be taken into account that anticipating the final structure around a galaxy is rather difficult given the dependence on the environment and merger history in the formation of each particular galaxy (Phillips et al. 2014).

Observationally, it is not uncommon to run into difficulties identifying and studying tidal structures around galaxies, sometimes these structures are too faint compared to the central light distribution that a detailed analysis proves impossible. Nevertheless, there are observations where faint structures such as shells are clearly seen around galaxies at some particular radii from the center of their associated host (Turnbull, Bridges & Carter 1999; Malin & Carter 1983; Buta et al. 2010; Laurikainen et al. 2010; Fort et al. 1986; Schweizer & Seitzer 2008). In some situations it has been possible to identify younger stellar populations in the outskirts compared to those in the inner bulge (Kang et al. 2009) probably reminiscent of a late gas accretion. It is worth noticing that in the CDM model the spatial location of these remnants of past interaction is not predicted and has to be tracked with numerical simulations as it depends on the history of each galaxy.

Metallicity is another powerful tool to constrain galaxy evolution across cosmic epochs as it is known to be correlated to gas infall, outflows due to supernovae, and star formation rate within the galaxy. Recent studies of star formation focused on local group dwarf galaxies (Weisz et al. 2014a,b) revealing radial gradients in metallicity (Kirby et al. 2013), and most of them seem to have old stellar populations formed ~ 10 Gyrs ago (Madau et al. 2014), followed by a more quiescent star formation likely due to loss of gas mass at the reionization epoch. There are high redshift galaxies ($z \sim 3$) that also show metallicity gradients, their regions of high star formation rate (SFR) are also of lower metallicity (Mannucci et al. 2009, 2010; Cresci et al. 2010) due to a large gas infall, they are surrounded by a more enriched disc, in Mannucci et al. (2010) the authors concluded that these observations are consistent with accretion of metal-poor gas in massive galaxies where a high SFR can be sustained without requiring frequent mergers,

this picture was also suggested by studies of gas rich disks at $z \sim 1-2$ (Fürster Schreiber et al. 2009; Tacconi et al. 2010).

In order to describe the debris around galaxies and stellar population it is necessary to include the gas dynamics in simulations, Even though there is an uncertainty due to our lack of understanding of the baryonic processes, their addition is also required to partially reduce some discrepancies of the CDM model, for instance, the cusp-core problem (see de Blok (2010) for a review), the overabundance of satellites (Klypin et al. 1999; Moore et al. 1999; Simon & Geha 2007; Belokurov et al. 2010; Macciò et al. 2012; Garrison-Kimmel et al. 2014) or the Too-Big-to-Fail (Boylan-Kolchin et al. 2011; Garrison-Kimmel et al. 2014b) issue. However, some of these discrepancies might also be solved assuming different properties for the dark matter, leading to for instance, scalar field dark matter (SFDM) (Sin 1994; Lee & Koh 1996; Guzmán & Matos 2000; Matos & Ureña 2001), strongly self-interacting DM (Spergel & Steinhardt 2000; Vogelsberger, Zavala & Loeb 2012; Colin et al. 2002; Rocha et al. 2013), warm dark matter (Bode, Ostriker & Turok 2001; Macciò et al. 2012).

It is of particular interest for us the SFDM alternative, here the mass of the field is assumed to be very small ($\sim 10^{-22} eV/c^2$) such that its de Broglie wavelength is of order \sim kpc, relevant for galactic scales. The quantum behavior of the field has created much interest in the model due to its success to account for some discrepancies mentioned above with dark matter properties only, for example, the small mass keeps the central density from increasing indefinitely due to the uncertainty principle in contrast to CDM simulations where supernova feedback is required (Governato et al. 2010, 2012; Pontzen & Governato 2012; Scannapieco et al. 2013), note that the amount of feedback required to produce a constant central density may be in conflict with other observations (Kuzio de Naray & Spekkens 2011; Peñarrubia et al. 2012; Boylan-Kolchin et al. 2014).

An interesting property that has been noted for scalar field haloes in excited states or in a superposition of them is the appearance of “ripples” in their mass density profiles (Seidel & Suen 1990; Balakrishna, Seidel, & Suen 1998; Guzmán & Ureña-López 2004; Ureña-López & Bernal 2010; Bernal et al. 2010; Matos & Ureña-López 2007; Robles & Matos 2013). This property motivated us to investigate whether features like rings or shells in non-interacting galaxies hosted by multistate scalar field haloes could arise independently of the galaxy merger mechanism.

In the next section we give a brief overview of previous works in the scalar field dark matter model and describe a model for galaxy formation in SFDM haloes. We modify the hydrodynamics code ZEUS to implement an evolving SFDM halo in which a gaseous component is present, we provide the details of our simulations in Section 3. In Section 4 we discuss our results and section 5 is devoted to our conclusions.

2 SFDM

2.1 Overview

The main idea in the scalar field dark matter model (Sin 1994; Ji & Sin 1994; Lee & Koh 1996; Guzmán & Matos

2000; Matos & Ureña 2001; Hu, Barkana, & Gruzinov. 2000) considers a self-interacting scalar field with a very small mass, typically of $\sim 10^{-22} \text{eV}/c^2$, such that the quantum mechanical uncertainty principle and the interactions prevent gravitational collapse in self-gravitating structures, thus the haloes are characterized with homogeneous densities (usually referred as a cores) in their centers, in general the core sizes depend on the values of the mass and the self-interacting parameters (Colpi, Shapiro, & Wasserman 1986) (for a review see Suárez, Robles & Matos (2013); Rindler-Daller & Shapiro (2014)).

There has been several studies of the cosmological evolution that results for a scalar field mass $m \sim 10^{-22} \text{eV}/c^2$, with this mass the cosmological density evolution of CDM can be reproduced (Matos & Ureña 2001; Chavanis 2011; Suárez & Matos 2011; Magaña et al. 2012; Schive, Chiueh, & Broadhurst 2014), there is consistency with the acoustic peaks of the cosmic microwave background radiation (Rodríguez-Montoya et al. 2010) and it implies a sharp cut-off in the mass power spectrum for halo masses below $10^8 M_\odot$ suppressing structure formation of low mass dark matter haloes (Marsh & Silk 2014; Bozek et al. 2014; Hu, Barkana, & Gruzinov. 2000; Matos & Ureña 2001). Moreover, there is particular interest in finding equilibrium configurations of the system of equations that describe the field (Einstein-Klein-Gordon system) and of its weak field approximation (Schrödinger-Poisson (SP) system), different authors have obtained solutions interpreted as boson stars or later as dark matter haloes showing agreement with rotation curves in galaxies and velocity dispersion profiles in dwarf spheroidal galaxies (Seidel & Suen 1991; Lee & Koh 1996; Böhmer & Harko 2007; Robles & Matos 2012, 2013; Lora et al. 2012; Lora & Magaña 2014; Martínez-Medina, Robles, & Matos 2015; Diez-Tejedor et al. 2014; Guzmán et al. 2014). So far the large and small scales observations are well described with the small mass and thus has been taken as a preferred value but the precise values of the mass and self-interaction parameters are still uncertain, we believe tighter constraints can come from numerical simulations (Schive, Chiueh, & Broadhurst 2014) and comparisons with large galaxy samples which we plan to do in the future.

Recently the idea of the scalar field has gained interest, given the uncertainty in the parameters the model has adopted different names in the literature depending on the regime that is under discussion, for instance, if the interactions are not present and the mass is $\sim 10^{-22} \text{eV}/c^2$ this limit was called fuzzy dark matter (Hu, Barkana, & Gruzinov. 2000) or more recently wave dark matter (Schive, Chiueh, & Broadhurst 2014), another limit is when the SF self-interactions are described with a quartic term in the scalar field potential and dominate over the mass (quadratic) term, this was studied in (Goodman 2000; Slepian & Goodman 2012) and called repulsive dark matter or fluid dark matter by (Peebles 2000).

Notice that for a scalar field mass of $\sim 10^{-22} \text{eV}/c^2$ the critical temperature of condensation for the field is $T_{\text{crit}} \sim m^{-5/3} \sim \text{TeV}$, which is very high, if the temperature of the field is below its critical temperature it can form a cosmological Bose-Einstein condensate, if it condenses it is called Bose-Einstein condensed (BEC) dark matter (Matos & Ureña 2001; Guzmán & Matos 2000;

Bernal et al. 2010; Robles & Matos 2013; Harko 2011; Chavanis 2011; Li et al. 2014). Sikivie & Yang (2009) mentioned that axions could also form Bose-Einstein condensates even though their mass is larger than the previous preferred value, notice that the result was contested in Davidson & Elmer (2013), this suggests that the condensation process should be studied in more detail to confirm it can remain as BEC dark matter. In Ureña-Lopez (2009), it was found that complex scalar field with $m < 10^{-14} \text{eV}/c^2$ that decoupled being still relativistic will always form a cosmological Bose-Einstein condensate described by the ground state wavefunction, this does not preclude the existence of bosons with higher energy, particularly in dark matter halos.

We see that the smallness of the boson mass is its characteristic property and cosmological condensation is a likely consequence. The preferred mass of the scalar field dark matter lies close to $\sim 10^{-22} \text{eV}/c^2$ satisfying the above constraint, although there are still uncertainties on the mass parameter, in order to avoid confusion with the known axion and help with the identification in future works, we find it useful and appropriate to name the scalar field dark matter candidate, given the above characteristics we can define it as a particle with mass $m < 10^{-14} \text{eV}/c^2$, being commonly described by its wavefunction we choose to name this DM candidate *psyon*.

It is worth emphasizing that despite the variety of names given to the model the main idea mentioned above remains the same, it is the quantum properties that arise due to the small mass of the boson that characterize and distinguish this paradigm, analogous to the standard cosmological model represented by the CDM paradigm whose preferred dark matter candidates are the WIMPs (weakly interacting massive particles), one being the neutralino, we see that all the above regimes SFDM, Repulsive DM, Axion DM, or any other model assuming an ultra light bosonic particle comprise a single class of paradigm, which we call *Quantum Dark Matter* (QDM) paradigm. As pointed before, in the QDM paradigm the small mass of the dark matter boson leads to the possibility of forming cosmological condensates, even for axions which are non-thermally produced and have masses in $10^{-3} - 10^{-6} \text{eV}/c^2$ (Sikivie & Yang 2009), from here we can obtain a characteristic property that distinguishes these dark matter candidates from WIMPs or neutrinos, namely, the existence of *bosons in the condensed state*, or simply *BICS*, from our above discussion the axion and psyon are included in the BICS.

2.2 Dark matter haloes of scalar field

There has been considerable work to find numerical solutions to the non-interacting SFDM in the non-relativistic regime to model spherically symmetric haloes (Guzmán & Ureña-López 2004; Ureña-López & Bernal 2010; Bernal et al. 2010; Bray 2012; Ruffini & Bonazzola 1969; Kaup 1968; Seidel & Suen 1991; Lee & Lim 2010), and also for the self-interacting SFDM (Böhmer & Harko 2007; Robles & Matos 2012; Colpi, Shapiro, & Wasserman 1986; Rindler-Daller & Shapiro 2012; Balakrishna, Seidel, & Suen 1998; Goodman 2000), it is worth noting that as mentioned in Guzmán & Ureña-López (2004) for the weak field limit of the system that determines the evolution of

a spherically symmetric scalar field, that is, the Einstein and Klein-Gordon equations, for a complex and a real scalar field the system reduces to the Schrödinger-Poisson equations (Arbey et al. 2003). From current bounds reported in Li et al. (2014) obtained by imposing that the SF behaves cosmologically as pressureless matter (dust) we obtained that the interacting parameter would be extremely small for the typical mass of $\sim 10^{-22} \text{eV}/c^2$, therefore we expect that solutions to the SP system with no interactions would behave qualitatively similar to those when self-interactions are included, this assumption is supported by the similarity in the solutions for a small self-coupling found in other works (Balakrishna, Seidel, & Suen 1998; Colpi, Shapiro, & Wasserman 1986; Briscese 2011), in this work we will study the non-interacting solutions.

One characteristic feature of stationary solutions of the form $\psi(\mathbf{x}, t) = e^{-iE_n t} \phi(r)$ for the SP system is the appearance of nodes in the spatial function $\phi(r)$, these nodes are associated to different energy states of the SF, the zero node solution corresponds to the ground state, one node to the first excited state, and so on. These excited states solutions fit rotation curves (RCs) of large galaxies up to the outermost measured data and can even reproduce the wiggles seen at large radii in high-resolution observations (Sin 1994; Colpi, Shapiro, & Wasserman 1986; Robles & Matos 2013). However, haloes that are purely in a single excited state seem to be unstable when the number of particles is not conserved (finite perturbations) and decay to the ground state with different decay rates (Guzmán & Ureña-López 2004; Balakrishna, Seidel, & Suen 1998), though they are stable when the number of particles is conserved (infinitesimal perturbations). The ground state solution is stable under finite perturbations and infinitesimal perturbations (Bernal et al. 2010; Seidel & Suen 1990), but has difficulties to correctly fit the rotation curves in large galaxies because its associated RC has a fast keplerian behavior shortly after reaching its maximum value unable to remain flat enough at large radii.

One way to overcome this problem was to consider that bosons are not in one state but instead coexist in different states within the halo, given our intention to describe dark matter haloes we will refer to such configurations as multistate halos (MSHs) (Ureña-López & Bernal 2010; Matos & Ureña-López 2007; Robles & Matos 2013, b). The size of the MSH is determined by the most excited state that accurately fits the RC for large radii, excited states are distributed to larger radii than the ground state, and in contrast to the halo with single state there are MSHs that are stable under finite perturbations provided the ground state in the final halo configuration has enough mass to stabilize the coexisting state (Ureña-López & Bernal 2010; Bernal et al. 2010). In Bernal et al. (2010) it was shown that MSHs can be studied in the classical approach as a collection of classical scalar fields coupled through gravity, one field ψ_i for each state, this would modify the SP system such that its source of energy density would be the sum of densities in each state (Ureña-López & Bernal 2010), where each state satisfies its respective Schrödinger equation and the states are coupled through the Newtonian gravitational potential U .

In spherical symmetry (in units $\hbar=1, c=1$) the SF solutions, Φ_n , satisfying the Einstein-Klein-Gordon system are

related to the SP wavefunctions through

$$\sqrt{8\pi G} \Phi_n(\mathbf{x}, t) = e^{-imt} \psi_n(\mathbf{x}, t) \quad (1)$$

with m the mass of the SF. For stationary solutions we can assume wavefunctions of the form $\psi_n(\mathbf{x}, t) = e^{-iE_n t} \phi(r)$, then the SP system reads

$$\begin{aligned} \nabla^2 \phi_n &= 2(U - E_n) \phi_n \\ \nabla^2 U &= \sum_n |\phi_n|^2 \end{aligned} \quad (2)$$

with ∇^2 the Laplacian operator in spherical coordinates, and E_n the energy eigenstates.

We consider the case of a MSH with only the ground and first excited states given that for this MSH Ureña-López & Bernal (2010) reported the critical value for its stability under small perturbations. If the ground state has $N^{(1)}$ particles and there are $N^{(2)}$ in the excited state, the authors found that MSH would be stable under small perturbations provided the fraction

$$\eta := \frac{N^{(2)}}{N^{(1)}} \leq 1.2 = \eta_{max}. \quad (3)$$

In all the configurations studied in which η is larger than the maximum for stability η_{max} , the induced instability causes the configuration to lose a few particles and a remarkable effect takes place, the excited state does a fast transition to the ground state and viceversa, that is, the populations of the states are inverted such that the final η complies with the stability condition (3), after the inversion the MSH approaches a stable configuration where the particle number remains constant for each state, after the transition the particles that were initially in the excited state are now in the ground state where they have redistributed and become more compact than in their original distribution.

This population inversion (PI) is a characteristic feature of MSHs and as we will show it can have consequences in the gas distribution and on the accretion rate during the period of galaxy formation. In fact, given the cut-off in the mass power spectrum due to the small mass of the psyon we expect a delay in the first structures to collapse compared to the those found in CDM (Matos & Ureña 2001; Marsh & Silk 2014; Bozek et al. 2014), this was confirmed with cosmological simulations for a mass of $8 \times 10^{-23} \text{eV}$ (Schive, Chiueh, & Broadhurst 2014), therefore, this intrinsic change of states within MSHs at high redshift might have observable consequences in the gas and stellar properties of the galaxies that will form in such potential wells.

2.3 Galaxy formation scenario in SFDM haloes

Initial fluctuations that grow due to the cosmological expansion of the universe eventually separate from it and start collapsing due to its own gravity, at this time (known as turnaround) the halo has a number of psyons that can be in different states, their values would be determined before the collapse of the configuration, and have some dependence on the its local environment. Depending on the number density of bosons populating the excited states we can have different fates for the haloes as mentioned in subsection (2.2).

From the mentioned results of the literature and based

on the successful fits to different galaxies we propose the following model of galaxy formation in SFDM haloes. The smallest and less dense systems, such as dwarf galaxies, would reside in SFDM haloes with most bosons in the ground state except possibly for just a few excited particles (Martinez-Medina, Robles, & Matos 2015), this is because the potential wells of these haloes, being the lowest dense systems, would be just massive enough to collapse and allow the existence of the state of minimum energy that would form a bound configuration. Larger configurations that had initially a larger number of bosons in excited states than in the ground state can undergo a population inversion and reach a stable state, collapse to a dense ground state or become a black hole depending on how large the fraction of particles in excited states is after turnaround, given the different possible outcomes for this case we expect that most galaxies are formed this way, for instance, ellipticals can form when haloes transition to a stable configuration to form a ground state and quickly deepen the gravitational potential resulting in a dense and compact structure where the bulge can form, for high surface brightness galaxies which usually have RCs that fall slowly after its maximum, these galaxies would likely correspond to SFDM haloes whose final stable configuration has a comparable number of bosons in the excited and ground states as both states would contribute evenly in the central region increasing the potential well where more star formation can take place, and for distances larger than a given radius (likely the first maximum peak in the RC) the ground state would be a small contribution to the density, thus in the outer region the baryonic RC would remain below its maximum. Another possible outcome for extended haloes is when the fraction of excited particles is below its stability threshold, here gravity will slowly redistribute DM bosons in the stable MSH but mostly keeping the particle number constant, considering that psyns in the excited states are subdominant but more widely distributed than the ones in the ground state of a MSH, the DM gravitational potential in the center would be less dense than in the high surface brightness case so that gas accretion would also proceed more slowly resulting in rotation curves for the baryonic matter that slowly increase to large radii or with almost flat profiles, this case is quite similar to what is found in low surface brightness galaxies (Kuzio de Naray et al. 2010; Kuzio de Naray & Spekkens 2011; Kuzio de Naray & Kaufmann 2011).

This galaxy formation scenario broadly describes the different galaxy types showing that only due to the dark matter properties in the context of SFDM it is possible to agree with the general features of several galaxies. However, we do not expect this scenario to represent all galaxies, in fact, to get a better description of individual galaxies we require taking into account other fundamental parameters that affect their evolution, such as the environment, angular momentum, galaxy mergers etc., we will leave a more in depth exploration of the scenario including the full astrophysical processes for a future work.

For now, we take the given description of elliptical galaxies to explore whether some substructure found in some of these galaxies can be a consequence of the properties of the background DM halo where such ellipticals are formed. We do not discard the possibility that shells or rings result

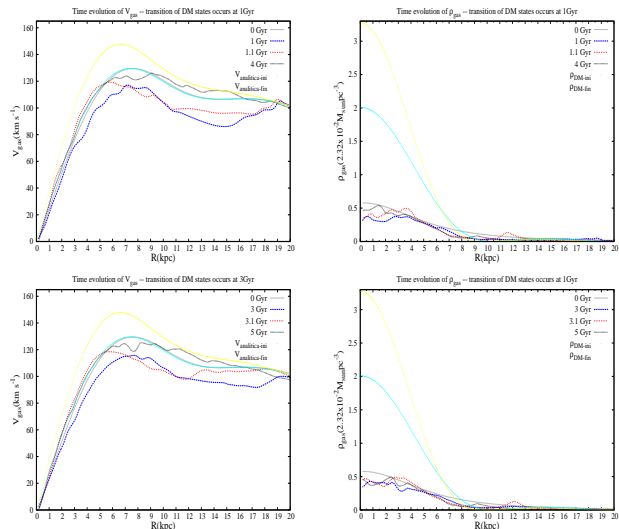


Figure 1. Density profiles for dark matter and gas for simulations A_1^1 (upper panels) and A_1^3 (lower panels). Shown are the initial (cyan lines) and final (yellow lines) DM profiles of the MSH composed of the ground and first states of the scalar field. Also shown are the initial condition for the disc of gas (gray lines), its density and rotation curve just before (blue-dashed line) and shortly after (red-dashed line) the population inversion occurs in the SFDM halo to reach its stable configuration, the black dashed line shows the profiles at the end of the simulations when the multistate halo is now stable.

from mergers, instead, we explore a new possible mechanism in which they can arise offering an alternative explanation to the tidal debris in certain non-interacting ellipticals. We study this issue in a multistate halo.

3 SIMULATIONS

We consider a multistate halo with only the first and ground state coexisting, this is because we know the stability threshold for this multistate configuration. In Bernal et al. (2010) it was seen that the larger the η above the critical value, the faster it settles to its final stable configuration, to be sure that the MSH is initially in the unstable regime we pick an intermediate value $\eta=1.6$. We explore the evolution of the gas distribution that follows a disc of gas with a Miyamoto-Nagai profile (Miyamoto & Nagai 1975) with gas mass of $M_g = 3.9 \times 10^9 M_\odot$, and for the horizontal and vertical scale-lengths we use $a = 6.5$ kpc and $b = 0.5$ kpc respectively (we also simulated some cases with the same gas mass but using an initial spherical Plummer profile but found no change in the main results, there was only a slight increase in the computation time, we then report only the cases for an initial disc of gas).

The code we use to evolve the gaseous component embedded in the MSH is the hydrodynamics code ZEUS-MP (Hayes et al. 2006). It is a fixed-grid time-explicit Eulerian code, we solve for the standard hydrodynamics equation for the baryonic component as in Martinez-Medina & Matos (2014), but here, we modify the code to allow for the evolution of a multistate dark halo that undergoes a transition as described below. In order to implement the population inversion in ZEUS we use a semi-analytical model that

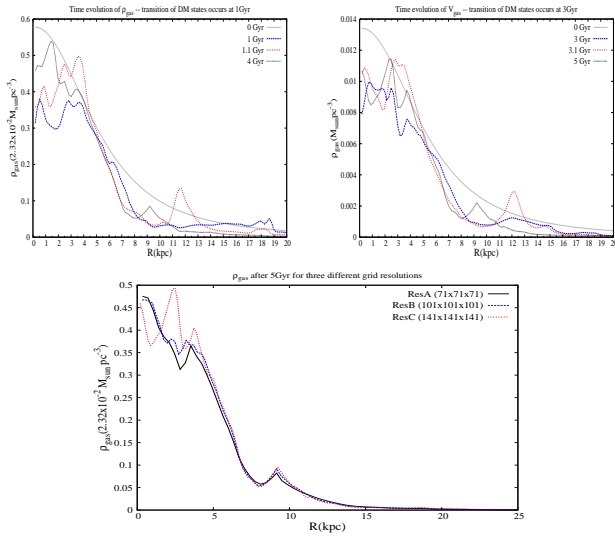


Figure 2. Density profiles for dark matter and gas for simulations A_1^1 (upper panels) and A_1^3 (lower panels). Shown are the initial (cyan lines) and final (yellow lines) DM profiles of the MSH composed of the ground and first states of the scalar field. Also shown are the initial condition for the disc of gas (gray lines), its density and rotation curve just before (blue-dashed line) and shortly after (red-dashed line) the population inversion occurs in the SFDM halo to reach its stable configuration, the black dashed line shows the profiles at the end of the simulations when the multistate halo is now stable.

let us control the rate of the transition to a stable state helping with the interpretation of the results. To achieve this we first use an analytical approximation to the numerical solutions obtained in the Newtonian limit for a confined distribution where the gravitational potential is weak (Ureña-López & Bernal 2010; Guzmán & Ureña-López 2004; Robles & Matos 2013), the scalar field density profile due to the wavefunction in the state j is

$$\rho_j(r) = \rho_{c,j} \frac{\sin^2(j\pi r/R_j)}{(j\pi r/R_j)^2}, \quad (4)$$

where $j=1+n$ labels the state of the scalar field and $n=0, 1, 2, \dots$ is the number of nodes in the profile, thus $j=1$ denotes the ground state with zero nodes and $j=2$ corresponds to the first excited state, and the total density of the MSH would be described by $\rho(r)=\rho_1(r)+\rho_2(r)$. In equation (4) $\rho_{c,j}$ represents the central density of state j and R_j is taken as a truncation radius of the corresponding state, that is, for radii greater than R_j the number of particles in the state j is neglected, thus we take $\rho_j(r)=0$ for all $r > R_j$ whereas for $r \leq R_j$ the density profile of the state j is given by (4).

The mass profile and rotation curve for state j are (Robles & Matos 2013; Martinez-Medina & Matos 2014)

$$M_j(r) = \frac{4\pi\rho_{c,j}}{k_j^2} \frac{r}{2} \left(1 - \frac{\sin(2k_j r)}{2k_j r} \right), \quad (5)$$

$$V_j^2(r) = \frac{4\pi G\rho_{c,j}}{2k_j^2} \left(1 - \frac{\sin(2k_j r)}{2k_j r} \right), \quad (6)$$

where we defined $k_j := j\pi/R_j$. The total mass enclosed

within R_j is

$$M_j(R_j) = \left(\frac{2}{\pi} \right) \frac{\rho_{c,j} R_j^3}{j^2}. \quad (7)$$

During the population inversion in the numerical solution both states lose a few percentage of their initial masses (<10% (Ureña-López & Bernal 2010; Bernal et al. 2010)), but this loss would not substantially affect the final halo profile, for this reason we will neglect the mass loss in our analytical study of the MSH. In order to construct the initial configuration in an unstable state we work with a mass ratio $\eta = 1.6$, when the population inversion occurs the initial mass ratio $M_2^i(R_2^i)/M_1^i(R_1^i)$ will also be inverted and the final MSH will be stable. After the inversion the total initial mass of the ground state $M_1^i(R_1^i)$ becomes the final mass of the excited state $M_2^f(R_2^f)$ and viceversa, and the nodes in the wavefunctions will also have changed, that is

$$M_1^i(R_1^i) \longrightarrow M_2^f(R_2^f), \quad M_2^i(R_2^i) \longrightarrow M_1^f(R_1^f) \quad (8)$$

$$j : 1, 2 \longrightarrow 2, 1 = j'. \quad (9)$$

We still need to specify a function to model the time evolution of the transition to the stable configuration. As we mentioned, for unstable haloes the transition happens really fast, during this period the central density varies until it reaches the new stable value, the inversion also modifies the radius of each state. In our semi-analytical approach the radius and density are related to the mass through eq.(7), thus we can choose to vary the radius to induce the transition, remembering that the transition is relatively fast, we found that a smooth function that captures the PI of the numerical evolution and allow an interpolation between an initial and final R_j is

$$R_{j'}^f(t) = R_j^i + \frac{\epsilon_{j',j}}{2} \left(1 + \tanh[\alpha(t - t_{inv})] \right), \quad (10)$$

where α determines the transfer rate from the initially unstable to the final stable MSH, $\epsilon_{j',j} = R_{j'}^f - R_j^i$ is a parameter that relates the initial radius to the one after the inversion, and t_{inv} is the time where the PI is halfway to reach its final stage with j' confined in $R_{j'}^f$, we applied a corresponding function to invert j to j' .

Using this semi-analytical inversion model we can identify and study the dependence of the resulting properties of the gaseous component on the transition time, in particular the effect on the production of tidal features. We modify the code ZEUS to implement the model and run simulations for a Miyamoto-Nagai disc of gas, the gas has no self-gravity and is used as a tracer of the gravitational potential, the initial condition for the gas velocities are set directly from the background dark matter halo and therefore match the initial halo velocities (see Fig. 1). As noted by other authors (Guzmán & Ureña-López 2004; Ureña-López 2002; Ureña-López, Valdez-Alvarado, & Becerril 2012) stationary solutions to the SP system (for a specified number of nodes) are related to each other by a scaling transformation, so the properties found here for our simulated parameters are expected to appear in similar configurations under a suitable scaling parameter. Table 1 shows the parameters of mass and radii for our MSH before and after the transition,

Table 1. Initial and final parameters defining the MSH.

	Initial		Final	
	j		j'	
	1	2	1	2
M^a	1.844	2.953	2.953	1.844
R^b	10	20	10	20

^a Mass in units $1 \times 10^{10} M_\odot$

^b Units in kpc

these are the values we will use that define the background MSH in all our runs, we explore an early and late transition specified by $t_{inv}=1$ and 3 Gyrs respectively, and we also evolve these cases when $\alpha = 1, 1/4$ corresponding to an fast and slow inversion, we denote by $A_\alpha^{t_{inv}}$ a realization that had a PI with parameters t_{inv} and α .

4 DISCUSSION

In Figure 1 we show the density profiles and the rotation curves for the MSH and the disc of gas comparing the cases of a rapid early and late transitions (A_1^1 and A_1^3). We notice the decline in the gas RC in both cases, in fact, the behavior is quite similar in both simulations, the gas moves according to the potential of the MSH and when the PI takes place it induces a rapid gas infall towards the center (see red dashed line in Fig.1) seen as an bulge like region of high gas density. In Figure 2 we plot a zoom to the gas densities of Figure 1 where we observe a conspicuous peak that appears as a result of the halo transition, soon after the transition a portion of the outer gas is pulled to the center and gets redistributed again in the now stable MSH configuration but now some of the gas remains trapped within the region of the first node of the MSH density profile, this results in the notable spike in the gas profiles. This density increase appears in both early and late fast transitions showing that this feature is expected independently of when the transition to the stable multistate halo happened. We verified that this is not a resolution effect by simulating A_1^3 for three different grid resolutions giving the density profiles shown in the bottom panel of Fig. 2, the inner profile does change due to the higher resolution that captures more details of the gas while the spike at ~ 9 kpc is only slightly modified and at the location of the node in the MSH, suggesting that its origin lies in the ripple-like feature of the background MSH.

This surprising agglomeration of gas at 9 kpc is nevertheless small compared to the mean central density ($\approx 0.45 M_\odot pc^{-3}$) being $\sim 20\%$ at the peak, the fact that it remains well after the transition is important for observations as this can be the origin of some structures around galaxies. In fact, in Fig. 3 we plot the gas spatial distribution at the beginning and at the end of the simulation with early and late halo transition, that is A_1^1 and A_1^3 , and we readily observe the presence of a surrounding ring of gas orbiting around the denser central concentration reminiscent of those found in certain elliptical galaxies. The ring keeps its location until the end of the simulations in our isolated galaxy

because its origin lies in the shape of the background SFDM halo, moreover, the stability of the halo under small perturbations, such as accretion of small galaxies, mildly change the inner DM potential but may alter the ring structure in a similar way that the population inversion modified the initial gas profile, however, once the merging process has concluded the gas will start redistributing and according to our results had enough gas remain on the outskirts a ring-like structure would appear again, the final amplitude of the ring's density will depend more strongly on the details of the merging process but its location should be similar to the non perturbed halo provided the DM halo potential was not severely modified, as expected for minor mergers in the past or those relatively more recent, thus, tidal features are not exclusive of galaxy mergers when the dark matter is an ultra light scalar field.

Comparing the early and late transitions in the MSH we obtain similar structures, thus we may focus on one of them, we choose the case of a late population inversion ($t_{inv}=3$ Gyrs) to explore the effect on the ring's shape under a fast ($\alpha=1$) and slow ($\alpha=1/4$) transition. Fig. 4 depicts the comparison at the end of the simulation, we observe that both A_1^3 and $A_{1/4}^3$ form the ring as expected but the slow transition spreads the gas around the ring creating a broader substructure, this is consistent with our galaxy formation scenario, as the gas accretion proceeds slower for $A_{1/4}^3$ the ring will slowly form from the concentration of consecutively infalling gas, on the other hand in A_1^3 the rapid transition enhances the gas infall and accelerates the gathering of gas at the ring's location quickly depleting the rest of the gas in low density regions creating a thin and more confined ring.

Moreover, a fast gas concentration is likely to induce a period of star formation, a massive accretion in the early universe would generate a starburst producing several stars and winds that could drive gas away from the center, part of the latter will be recycled and some can be trapped in the location where the outer ring forms, there the gas can trigger star formation too or just accumulate as dust, the central star formation affects the metallicity in that region and if the gas infall stops early due to effective gas blowouts consequence of a high star formation rate the galaxy would be left with a dominant fraction of old stars. For a massive galaxy, part of the ejected gas cannot escape and will remain bounded scattering the inner photons and producing a luminous bulge, this is consistent with the formation of some ellipticals, in particular this picture could describe the puzzling origin of dust rings in the Sombrero galaxy (M104) (Bajaja et al. 1984; Emsellem 1995), although a more careful study of this issue has to be done.

The gas fraction and nature of the dark matter halo are fundamental to determine the fate of a galaxy, for instance, dwarf galaxies reside in SFDM haloes in the ground state and have shallow potentials, then if a starburst occurs early it can blow out a large portion of gas that if it is accreted much later the next generations of stars will differ from the old population observed as two different fractions of stellar population where the younger one is located at larger radii due to its late accretion, analyses of stellar age and metallicity at different radii can be a way to distinguish between CDM predictions and the SFDM, future hydrodynamics simulations of SFDM will be able to confirm these predictions.

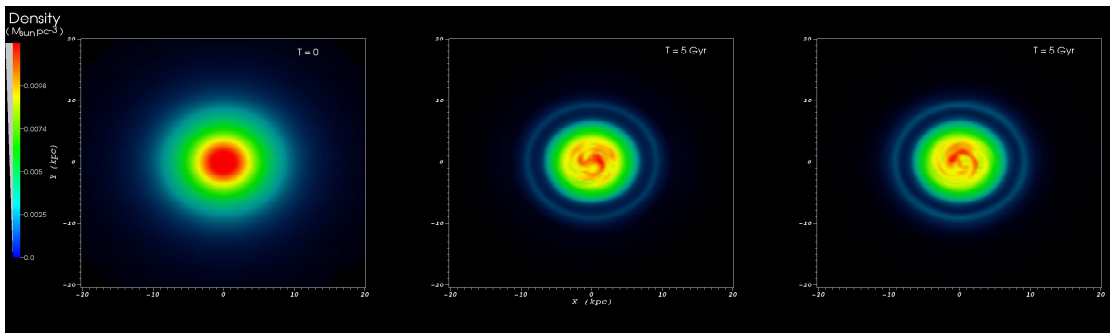


Figure 3. Comparison of initial gas distribution(left) and its final stage. The central panel corresponds to a halo that had an early transition to its stable configuration at $t_{inv}=1$ Gyr(A_1^3) and on the last panel(right) the transition was at a later epoch $t_{inv}=3$ Gyrs(A_1^3). A ring appears in both simulations at the corresponding density peak of Fig. 2.

The existence of the ring is a generic feature in our simulations of isolated galaxies, notice that for an initially stable halo ($\eta < \eta_{max}$) the ring will also appear, it suffices to observe that our final MSHs fall precisely in this regime. The SFDM model provides a new mechanism to form rings without major changes to the galaxy inner region mainly because it is where the ground state is mostly confined, in fact, the latter can exhibit a solitonic behaviour keeping its profile even after several mergers as shown in SFDM cosmological simulations (Schive et al. 2014b). Although perfect rings are created in our simulations, we note that this structure can be deformed by the passage of an accreted satellite or due to tidal forces from nearby galaxies culminating in incomplete or displaced rings, these tidal debris would manifest in the more common shells (Malin & Carter 1980, 1983; Turnbull, Bridges & Carter 1999).

Galaxies that undergo major mergers form under violent conditions, thus the shape of their tidal structures can vary widely especially when the interaction is still ongoing, for these latter galaxies far from equilibrium the emergence of an exotic tidal feature might be more accurately explained by modeling the merging galaxy and evolving it in a simulation that includes baryonic processes and a live halo. For the more isolated systems like the considered here, we have found that there is another mechanism that leads to outer structures but with the difference that they possess a certain degree of symmetry associated to the background DM halo and not to a particular merger event.

It is interesting that the quantum properties of the pysons manifest on a macroscopic scale and have implications in observable quantities like gas and stars, remarkably a similar situation where quantum effects manifest on larger scales has already been observed in local experiments, in particular it was seen that water droplets can bounce indefinitely on the surface of a vibrating fluid bath and propel themselves across the surface of the fluid by virtue of their pilot-wave dynamics exhibiting quantum features like single-particle diffraction, tunneling, quantized orbits, and orbital level splitting (Walker 1978; Couder et al. 2005; Couder & Fort 2006; Protiere, Boudaoud, & Couder

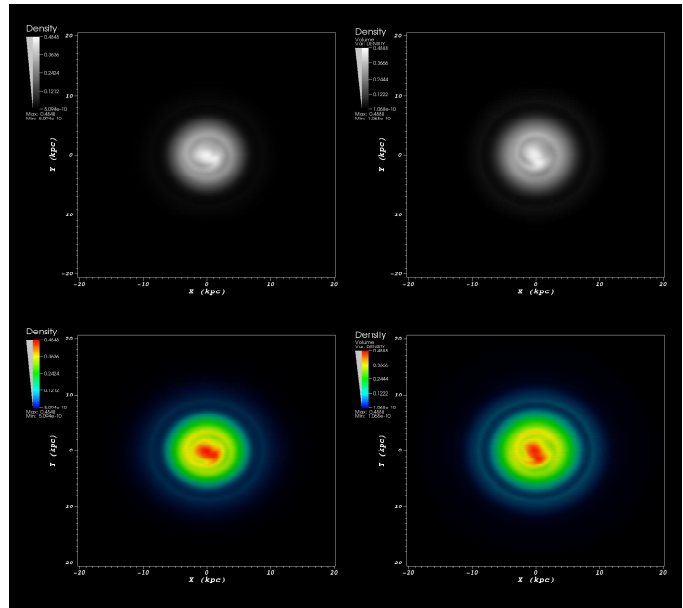


Figure 4. Gas distribution after 5 Gyrs for simulations A_1^3 (upper-left and its colored scale in the bottom-left panel) and $A_{1/4}^3$ (upper-right and its colored version in the bottom-right panel). The ring on the left panels is more defined as the MSH undergoes a rapid transition to stability while for a slow transition (right panels) more particles are spread around the ring.

2006; Eddi et al. 2009, 2012; Fort et al. 2010; Bush 2010; Ozaa, Rosales, & Bush 2013). In the SFDM context the analogue fluid would be the dark matter and the baryons would be the droplets guided by the DM, whether this analogy is valid deserves further consideration and will be treated in other work.

5 CONCLUSIONS

In this work we have seen that if the dark matter is a ultra light scalar field the internal structure of galaxies can reflect fossil records of their formation, in our case we study the formation of tidal structures similar to rings and shells in non-interacting galaxies. We discussed the nature of these structures in the context of SFDM and conclude that independently of galaxy mergers they can arise as a consequence of the quantum nature of the scalar field dark matter boson (hereafter *psyons*) that form the halo where galaxies are embedded in, mainly, due to the intrinsic ripples in the dark matter halo density profile.

The possibility of describing tidal substructure in scalar field dark matter halos was also suggested in Bray (2012) but under different halo configurations and without including the evolution of a gaseous component, here we make use of spherically symmetric haloes in multistates because their stability has been studied and confirmed in previous works (Ureña-López & Bernal 2010; Bernal et al. 2010). In addition, they possess desirable properties to describe a variety of galaxies. Inspired by the numerical solutions in Ureña-López & Bernal (2010), where they reported the maximum fraction of psyons in excited states (eq. 3) to form a stable multistate halo composed of the ground state and first excited state, we propose a semi-analytical model to describe a similar halo configuration and study the distribution of a gaseous disc that is contained within such scalar field DM halo. The halo is set to be initially unstable by choosing a fraction of excited boson above the stability limit, this induces a transition to reach a final stable configuration affecting the initial gas distribution, after the transition the population of the states is inverted and the halo stabilizes once the ground state dominates the halo mass that by gravity will be confined later in the center of the halo. At the end of the simulations (5 Gyrs) part of the gas keeps orbiting in the form of a ring outside the main bulge-like region, the structure of the ring is not significantly different when the halo transition happens early ($t_{inv}=1$ Gyrs) or late ($t_{inv}=3$ Gyrs) but the ring broadens if the transition is slow and becomes more defined for fast transitions. Due to the lack of stability parameter for MSH in higher energy states we explore the first non trivial superposition of multistates, given the positive results it seems that tidal structures would also be found at larger radii for SFDM haloes that have boson in higher excited states, although they would become fainter with distance, this would agree with shells that appear to be distributed at larger radii.

The tidal features in this work have a distinct origin from the usual tidal stripping of galaxies, they emerge from the quantum properties of the psyons that compose the dark halo, the presence of the symmetric ring is due to the spherically symmetry hypothesis, deviations from this symmetry could result in incomplete rings and shells although a certain degree of symmetry should remain which distinguishes to remnants that come from recent galaxy mergers that depend on the path of the accreted satellites and does not necessarily leave tidal debris of a particular symmetry, our results suggest that outer regions of dark haloes may not be totally smooth. Exploring in more detail the regions where shells and rings form could also help to put constraints on their origin, their formation, and serve to test galaxy and

halo formation scenarios such as the quantum dark matter (QDM) paradigm.

Additionally, we have provided a classification for the dark matter models that are based on the assumption that the dark matter is a scalar field of a very small mass that proves useful for future references and that helps to establish the main feature of the particle candidates of this paradigm. We formulate a galaxy formation scenario based on known results of halo formation in the SFDM context that can explain qualitatively the general properties of the different galaxy types in the universe and applied to interpret our findings. Given the success of the SFDM model to account for the apparent discrepancies of the standard CDM model with only dark matter properties, it will be desirable to include astrophysical processes in simulations to get a fair comparison with state-of-the-art CDM simulations. The QDM paradigm is indeed an interesting possibility that deserves further study.

ACKNOWLEDGMENTS

This work was partially supported by CONACyT México under grants CB-2009-01, no. 132400, CB-2011, no. 166212, and I0101/131/07 C-234/07 of the Instituto Avanzado de Cosmología (IAC) collaboration (<http://www.iac.edu.mx/>). Victor H. Robles and L. Medina are supported by a CONACyT scholarship.

REFERENCES

- Arbey A., Lesgourgues J., & Salati P., 2003, PRD, 68, 023511
- Bajaja E., van der Burg G., Faber S.M., et al., 1984, AA, 141, 309-317
- Balakrishna J., Seidel E., & Suen W.-M., 1998, PRD, 58, 104004
- Barnes J.E., Hernquist L., 1992, Annual Review of Astronomy and Astrophysics, 30, 705
- Behroozi P.S., Risa H. Wechsler R.H., Wu H.Y., 2013, ApJ, 763, 18
- Belokurov, V., Walker, M. G., Evans, N. W. et al., 2010, ApJ, 712, L103
- Bendo G.J., Buckalew B.A., Dale D.A., Draine B.T. et al. 2006, ApJ, 645, 134
- Bernal A., Barranco J., Alic D., & Palenzuela C., 2010, PRD, 81, 044031
- Bode P., Ostriker J.P., Turok N., 2001, ApJ, 556, 93
- Böhmer C.G., & Harko T., 2007, JCAP06, 025
- Boylan-Kolchin, M., Bullock, J. S., Kaplinghat, M. 2011, MNRAS, 415, L40
- Boylan-Kolchin M., Bullock J.S., Garrison-Kimmel S., 2014, MNRAS, 443, L44
- Bozek B., Marsh D.J.E., Silk J., Wyse R.F.G., 2014, arXiv:1409.3544
- Bray H.L., 2012, arXiv:1212.5745
- Briscese F., 2011, Phys.Lett.B, 696, 315
- Bush J.W.M., 2010, Proc. Nat. Acad. Sci., 107, 17455
- Buta R.J., Sheth K., Regan M. et al., 2010, ApJS, 190, 147
- Chavanis P.H., 2012, A&A 537, A127

- Colin P., Avila-Reese V., Valenzuela O., Firmani C., 2002, *ApJ*, 581, 777
- Colpi M., Shapiro S.L., & Wasserman I., 1986, *PRL*, 57, 2485
- Couder Y., Fort E., Gautier C.H., & Boudaoud A., 2005, *PRL*, 94, 177801
- Couder Y., & Fort E., 2006, *PRL*, 97, 154101
- Cresci G., Mannucci F., Maiolino R. et al., 2010, *Nature*, 467, 811
- Davidson S., & Elmer M., 2013, *JCAP12*, 034
- de Blok W.J.G., 2010, *Advances in Astronomy*, Article ID 789293
- Diez-Tejedor A., Gonzalez-Morales A.X., & Profumo S., PRD, 2014, 90, 043517
- Eddi A., Fort E., Moisy F., & Couder Y., 2009, *PRL*, 102, 240401
- Eddi A., Moukhtar J., Perrard S., Fort E., & Couder Y., 2012, *PRL*, 108, 264503
- Emsellem, E., 1995, *AA*, 303, 673
- Förster Schreiber N.M., Genzel R., Bouché N. et al., 2009, *ApJ*, 706, 1364
- Fort, B. P., Prieur, J.-L., Carter, D., Meatheringham, S. J., & Vigroux, L. 1986, *ApJ*, 306, 110
- Fort E., Eddi A., Boudaoud A. et al., 2010, *Proc. Nat. Acad. Sci.*, 107(41), 17515
- Garrison-Kimmel, S., Boylan-Kolchin, M., Bullock, J. S., Lee, K. 2014, *MNRAS*, 438, 2578
- Garrison-Kimmel, S., Boylan-Kolchin, M., Bullock, J. S., Kirby, E. N. 2014, *MNRAS*, 444, 222
- Governato F., Brook C., Mayer L. et al., 2010, *Nature*, 463, 203
- Governato F., Zolotov A., Pontzen A. et al., 2012, *MNRAS*, 422, 1231
- Goodman J., 2000, *New Astronomy* 5, 103
- Guzmán F.S., Lora-Clavijo F.D., González-Avilés J.J., & Rivera-Paleo F.J., 2014, *PRD*, 89, 063507
- Guzmán F.S., & Ureña-López L.A., 2004, *PRD*, 69, 124033
- Guzmán, F. S., & Matos, T. 2000, *Class. Quant. Grav.*, 17, L9
- Harko T., 2011, *PRD*, 83, 123515
- Hau G.K.T., & Forbes D.A., 2006, *MNRAS*, 371, 633
- Hayes J.C., Norman M.L., Fiedler R.A., 2006, *ApJS*, 165, 188.
- Hu W., Barkana R., Gruzinov A., 2000, *PRL*, 85, 1158
- Ji S.U., & Sin S.J., 1994, *PRD*, 50, 3655
- Kang M., Biegging J. H., Kulesa C.A., Lee Y., 2009, *ApJ*, 701, 454
- Kaup D.J., 1968, *Phys. Rev.*, 172, 1331
- Kirby E.N., Cohen J.G., Guhathakurta P. et al., 2013, *ApJ*, 779, 102
- Klypin A.A., Trujillo-Gomez S., Primack J., 2011, *ApJ*, 740, 102
- Klypin, A., Kravstov, A. V., Valenzuela, O., Prada, F. 1999, *ApJ*, 522, 82
- Koprolin, W., Zeilinger, W., 2000, *A&A*, 145, 71
- Kuzio de Naray R., & Spekkens K., 2011, *ApJ*, 741, L29
- Kuzio de Naray R., & Kaufmann T., 2011, *MNRAS*, 414, 3617
- Kuzio de Naray R., Martinez G.D., Bullock J.S., & Kaplinghat M. et al., 2010, *ApJ*, 710, L161
- Laurikainen E., Salo H., Buta R., Knapen J.H., & Comerón S., 2010, *MNRAS*, 405, 1089
- Lee J.W., & Koh I.G., 1996, *PRD*, 53, 2236
- Lee J.W., & Lim S., 2010, *JCAP01*, 007
- Li B., Rindler-Daller T., & Shapiro P.R., 2014, *PRD*, 89, 083536
- Lora V., Magaña J., Bernal A., Sánchez-Salcedo F.J., & Grebel E.K., 2012, *JCAP02* (2012) 011
- Lora V., Magaña J., 2014, *JCAP09*, 011
- Macciò, A. V., Paduroin, S., Anderhalden, D. et al., 2012, *MNRAS*, 424, 1105
- Madau P., Weisz D.R., Conroy C., 2014, *ApJ*, 790, L17
- Magaña J., Matos T., Suárez A., Sánchez-Salcedo F.J., 2012, *JCAP* 1210, 003
- Mannucci F., Cresci G., Maiolino R. et al., 2010, *MNRAS*, 408, 2115
- Mannucci F., Cresci G., Maiolino R. et al., 2009, *MNRAS*, 398, 1915
- Malin, D. F. & Carter, D. 1983, *ApJ*, 274, 534
- Malin, D. F. & Carter, D. 1980, *Nature*, 285, 643
- Marsh D.J.E., & Silk J., 2014, *MNRAS*, 437, 2652
- Martínez-Delgado D., Peñarrubia J., Gabany R.J., Trujillo I. et al. 2008, *ApJ*, 689, 184
- Martínez-Delgado D., Pohlen M., Gabany R.J., Majewski S.R. et al., 2009, *ApJ*, 692, 955
- Martínez-Delgado D., Gabany R.J., Crawford K., Zibetti S. et al., 2010, *The Astronomical Journal*, 140, 962
- Martinez-Medina L.A., & Matos T., 2014, *MNRAS*, 444, 185
- Martinez-Medina L.A., Robles V.H., & Matos T., 2015, *PRD*, 91, 023519
- Matos, T., & Ureña-López, L. A. 2001, *Phys. Rev. D*, 63, 063506
- Matos T., Ureña-López L.A., 2007, *Gen. Relativ. Gravit.*, 39, 1279
- Michard, R. & Prugniel, P. 2004, *AA*, 423, 833
- Miyamoto M., & Nagai R., 1975, *PASJ*, 27, 533
- Moore, B., Ghigna, S., Governato, F. et al., 1999, *ApJ*, 524, L19
- Ozaa A.U., Rosales R.R., & Bush J.W.M., 2013, *Journal of Fluid Mechanics*, 737, 552
- Peebles P.J.E., 2000, *ApJ*, 534, L127,
- Peñarrubia J., Pontzen A., Walker M.G., Kozlov S.E., 2012, *ApJ*, 759, L42
- Phillips J.I., Wheeler C., Boylan-Kolchin M. et al., *MNRAS*, Volume 437, 1930
- Pontzen A., & Governato F., 2012, *MNRAS*, 421, 3464
- Protiere S., Boudaoud A., & Couder Y., 2006, *J. Fluid Mech.*, 554, 85
- Rindler-Daller T., Shapiro P.R., 2012, *MNRAS*, 422, 135
- Rindler-Daller T., & Shapiro P.R., 2014, *Mod. Phys. Lett. A*, 29, 1430002
- Robles V.H., & Matos T., 2013, *ApJ*, 763, 19
- Robles V.H., & Matos T. 2013b, *Phys. Rev. D* 88, 083008
- Robles V.H., & Matos T., 2012, *MNRAS*, 422, 282
- Rocha M., Peter A.H.G., Bullock J.S. et al., 2013, *MNRAS*, 430, 81
- Rodríguez-Montoya I., Magaña J., Matos T., Pérez-Lorenzana A., 2010, *ApJ*, 721, 1509
- Ruffini R., & Bonazzola S., 1969, *Phys. Rev.*, 187, 1767
- Scannapieco C., Wadepuhl M., Parry O.H. et al., 2012, *MNRAS*, 423, 1726
- Schive H.Y., Chiueh T., & Broadhurst T., 2014, *Nature*, 10, 496

- Schive H.Y., Liao M.H., Woo T.P., et al. 2014b, arXiv:1407.7762
- Schweizer, F. & Seitzer, P. 1992, AJ, 104, 1039
- Schweizer F. & Seitzer P., 1988, ApJ, 328, 88
- Seidel E., & Suen W-M., 1990, PRD, 42, 384
- Seidel E., & Suen W.M., 1991, PRL, 66, 1659
- Sikivie P., Yang Q., 2009, PRL, 103, 111301
- Simon, J. D., & Geha, M. 2007, ApJ, 670, 313
- Sin S.J., 1994, PRD, 50, 3650
- Slepian Z., & Goodman J., 2012, MNRAS, 427, 839
- Spergel D.N., Steinhardt P.J., 2000, PRL, 84, 3760
- Suárez A., Robles V.H., Matos T., 2014, Astrophysics and Space Science Proceedings, 38, 107
- Suárez A., & Matos T., 2011, MNRAS, 416, 87
- Tacconi L.J., R. Genzel R., Neri R. et al., Nature, 463, 781
- Taehyun K., Sheth K., Hinz J.L. et al., 2012, ApJ, 753, 43
- Turnbull, A. J., Bridges, T. J., & Carter, D. 1999, MNRAS, 307, 967
- Ureña-Lopez L.A., 2002, Class. Quant. Grav., 19, 2617
- Ureña-Lopez L.A., 2009, JCAP01, 014
- Ureña-López L.A., & Bernal A., 2010, PRD, 82, 123535
- Ureña-Lopez L.A., Valdez-Alvarado S., Becerril R., 2012, Class.Quant.Grav., 29, 065021
- van Dokkum, P. G. 2005, AJ, 130, 2647
- Vogelsberger M., Zavala J., Loeb A., 2012, MNRAS, 423, 3740
- Walker J., 1978, Scientific American, 238, 151
- Weisz D.R., Dolphin A.E., Skillman E.D. et al., 2014a, ApJ, 789, 147
- Weisz D.R., Dolphin A.E., Skillman E.D. et al., 2014b, ApJ, 789, 148